THE AMERICAN SOCIETY OF MECHANICAL ENGINEERS
345 E. 47th St., New York, N.Y. 10017

94-GT-476

A STUDY OF THE UNSTEADY PRESSURE OF A CASCADE NEAR TRANSONIC FLOW CONDITION

H. M. Atassi, J. Fang, and P. Ferrand*
Department of Aerospace and Mechanical Engineering
University of Notre Dame
Notre Dame, Indiana

Abstract

The rise of the unsteady pressure magnitude along the surface of a cascade blade in unsteady transonic flow is examined. It is shown that a similar rise in the unsteady pressure may occur for high subsonic flows where the mean flow is near sonic condition. For a subsonic cascade this unsteady pressure bulge is found to be associated with the cut-on of a new acoustic mode in the upstream direction. The level of the pressure bulge is significantly reduced as a downstream propagating mode cuts on. It is therefore proposed that this phenomenon is the result of the *blockage* of upstream propagating acoustic waves by the transonic mean flow. A transonic convergent-divergent nozzle is used as a model for investigating the *acoustic blockage* effect. Analytical and numerical computations using unsteady nonlinear Euler equations are then carried out to analyze and quantify the upstream and dowstream propagation of acoustic disturbances in the nozzle. The results confirm the sharp rise in the pressure of the upstream propagating disturbances at the nozzle throat as a result of the *acoustic blockage*.

1. Introduction

Experimental and computational studies have shown that the unsteady pressure distribution along the surface of an airfoil or of a cascade blade in unsteady transonic flow exhibits a significant bulge near the shock location. This pressure rise gives a significant contribution to the overall unsteady lift and moment. It also affects the flutter boundary of the airfoil or blade system and causes large local stresses which may result in high cycle fatigue failure. For a single airfoil, this phenomenon was examined by Tijdeman (1977) and Davis and Malcom (1979 and 1980). Tijdeman and Seebass (1980) reported that the unsteady pressure bulge and its phase variation resulted from nonlinear interaction between the mean and unsteady flows. This nonlinear interaction caused a shift in the shock position which cannot be predicted by thin airfoil theory.

In a recent review paper, Atassi (1994) reported linear and nonlinear Euler computations by Verdon, Huff and Ayer (1993) for subsonic and transonic cascades in oscillatory motion. The cascades have the geometry of the *Tenth Standard Configuration* (Fransson and Verdon, 1993). The linear calculations were obtained using LINFLO, a linearized unsteady aerodynamic code developed by Verdon and Hall (1990). The nonlinear computations were obtained from NPHASE, a fully nonlinear unsteady flow code developed by Huff et al. (1991). Two cases were considered. First a subsonic case where the upstream mean flow Mach number was 0.7, and a transonic case where the upstream mean flow Mach number was 0.8. Figure 1 shows the blade surface Mach number distribution for the transonic flow. It is seen that a shock occurs on the blade suction surface just ahead of the quarter chord point. The magnitude of the first harmonic unsteady pressure difference distribution for the cascade undergoing an in-phase torsional oscillation at a reduced frequency $k_1 = 0.5$ is shown in Figures 2 and 3 for the subsonic and transonic cases, respectively. It is significant to note the large rise in the magnitude of the unsteady pressure difference for the transonic case near the location of the mean flow shock. Similar unsteady pressure patterns were obtained by Ferrand (1986) using an unsteady Euler code for an airfoil oscillating in a transonic flow between two walls. For the subsonic case, Figure 3 shows that the maximum unsteady pressure is located near the leading edge where the mean flow quantities have large gradients. However, recent computational results by Atassi et al. (1993) for a cascade in a gust in high subsonic flow show a large rise in the unsteady pressure where the mean flow is close to critical sonic condition.

The present paper examines this unsteady pressure rise phenomenon and presents a physical explanation based on the fact that when the mean flow Mach number is close to unity, upstream propagating acoustic disturbances are blocked and strongly amplified. In this paper, this phenomenon will be referred to as *acoustic blockage*. A study of the unsteady surface pressure for two cascade geometries in a gust is first carried out for increasing but subsonic mean flow Mach numbers. Analytical and numerical models, using nonlinear Euler computations, are then developed for the *acoustic*

*Permanent address: Laboratoire de Mécanique des Fluides et d'Acoustique, URA 263, Ecole Centrale de Lyon, Ecully, France.

Presented at the International Gas Turbine and Aeroengine Congress and Exposition
The Hague, Netherlands — June 13–16, 1994

blockage effect in a nozzle to investigate and quantify this basic physical phenomenon.

2. Cascade Near Transonic Speed in A Gust

In the present paper, we consider cascades of airfoils in nonuniform flows. The upstream mean flow is assumed to he uniform and subsonic. Vortical disturbances known as gusts will be superimposed on this mean flow. An inviscid numerical code CASGUST, based on the analysis wherein the unsteady flow is linearized about the mean flow, was developed hy Fang and Atassi (1993a, 1993b). CASGUST calculates all unsteady flow quantities for impinging three-dimensional harmonic gusts of the form

$$u_{\infty}^{\rightarrow} = \vec{a} e^{i(\omega t - \vec{k}\cdot\vec{x})} \tag{1}$$

where $\vec{a} = \{a_1, a_2, a_3\}$ is the gust magnitude, ω is the frequency, t is time, $\vec{x} = \{x_1, x_2, x_3\}$ is the position vector where the x_1 axis is aligned with the upstream mean velocity $\vec{U}_{\infty}$, and $\vec{k} = \{k_1, k_2, k_3\}$ is the gust wave number vector. The cascade blades have a chord length c, and all lengths will be nondimensionalized with respect to c/2. The gust is assumed to he convected by the mean flow and thus $k_1 = \omega c/2U_{\infty}$ is the usual reduced frequency. The unsteady pressure p' will be nondimensionalized with respect to $\rho U_{\infty} a_2$.

Two cascade geometries are considered. Each is investigated for two Mach numbers and thus four flow cases are analyzed. The larger Mach numbers considered were such that the maximum Mach number on the blade suction surface M_{max} was just below unity. We first considered a lightly loaded cascade of cambered NACA 0006 blades. The camber line is a circular-arc with height at mid-chord of 5% of chord, the stagger angle $\chi = 15°$ and spacing $s/c = 1$. For case 1, the upstream mean-flow Mach number is $M_{\infty} = 0.74$ and the incoming and exit flow angles are $\Omega_{-\infty} = 25°$ and $\Omega_{+\infty} = 8.5°$, respectively. For case 2, we have $M_{\infty} = 0.70$ and $\Omega_{-\infty} = 25°$ and $\Omega_{+\infty} = 8.4°$. Figure 4 shows the cascade geometry and the Mach number contours. The maximum Mach number, for case 1, $M_{max} = 0.99$ occurs at ahout 20% of the chord from the leading edge on the hlade suction surface. For case 2, $M_{max} = 0.90$.

The other cascade geometry is an exit guide vane (EGV) cascade operating at high subsonic (case 3) and low subsonic (case 4) conditions. The blade of the EGV cascade has a thickness distribution of a NACA 0012 airfoil on a circular arc camber line with height at midchord of 13 percent of the chord c. The cascade spacing is $s/c = 0.6$, and its stagger angle $\chi = 15$ deg. The inlet flow angle is 40 deg. For case 3, $M_{\infty} = 0.61$, $M_{max} = 0.99$ again occurs at about 20% of the chord from the leading edge on the blade suction surface. For case 4, $M_{\infty} = 0.3$, and $M_{max} = 0.415$ also occurs at about 20% of the chord from the leading edge. The cascade geometry and the mean flow Mach number contours for case 3 are shown in Figure 5. The upstream vortical disturbances for all four cases are transverse gusts, i.e., $\{a_1 = 0, a_2 = 1, a_3 = 0\}$, and $\{k_2 = 0, k_3 = 0\}$. The reduced frequency k_1 is varied from 0 to 8.

Figure 6 shows the magnitude of the unsteady pressure distribution along the suction surface of the blade for cases 1 and 2 at $k_1 = 2.5$. For case 1, the unsteady pressure distribution exhibits a sharp peak where the mean-flow Mach number approaches its maximum value $M_{max} = 0.99$, close to unity. The peak value is more than 3 times larger than that of case 2 where $M_{max} = 0.90$. Figure 7 shows the magnitude of the unsteady pressure distribution for cases 3 and 4 at $k_1 = 4.35$. We equally note the large peak occuring in the unsteady pressure magnitude near sonic condition.

We conjecture that this sharp rise in the magnitude of the unsteady pressure is due to the near-sonic local flow condition. The near-sonic velocity acts as a barrier preventing acoustic disturbances from propagating upstream in a similar way to the shock for the transonic case shown in Figure 1 and 3. This *acoustic blockage* hy the local mean flow causes a significant rise in the magnitude of the unsteady pressure. For cases 2 and 4, the local Mach numbers are below unity and there is no similar rise in the magnitude of the pressure except at the leading edge.

In order to investigate whether this phenomenon occurs at all reduced frequencies, we have calculated the peak of the pressure magnitude in the region where M_{max} occurs. These results are shown in Figures 8 and 9 for case 1, and case 3, respectively. Figure 10 shows contours of the unsteady pressure magnitude versus the reduced frequency along the blade suction surface for case 1. For case 1, we note that the peaks in pressure are significantly higher in the range $1.4 < k_1 < 2.6$. As we examined the acoustic modes of the cascade, we found that at $k_1 = 1.4$, a second acoustic mode cuts on upstream and the cascade now is radiating two acoustic modes upstream and only one acoustic mode downstream. At $k_1 = 2.6$ a second acoustic mode cuts on downstream and the cascade now is radiating two acoustic modes both upstream and downstream. This infers that when there are more acoustic modes propagating upstream than downstream, the upstream propagation of the acoustic energy produced by the aft portion of the blades is blocked by the local near sonic flow condition. This local *blockage effect* causes a rise in the unsteady pressure as the acoustic waves move around this region of near sonic velocity. When a downstream modes cuts on, the rise in the unsteady pressure is not as significant as the acoustic waves now travel downstream.

A similar study for the unsteady pressure peaks for the EGV cascade shows a more complex pattern. Figure 9 shows a significant rise in the value of the pressure peaks in the range $2 < k_1 < 5$. At $k_1 = 2.8$ the first upstream propagating mode cuts on, while at $k_1 = 4.35$, the first downstream propagating mode cuts on. The location of the M_{max} is also shown about $0.20c$. The fact that the range for the high pressure peaks extend slightly beyond the cut-on range for the first upstream and downstream modes, can be explained by the increase in the unsteady pressure prior to the cut-on of an acoustic mode and to the large gradient of the mean-flow.

3. Model for the Acoustic Blockage

The flow in a cascade of airfoils is usually quite complex. The unsteady flow interacts with the mean flow which exhibits strong variations near the leading and trailing edges. It is also affected in a significant way by the cascade stagger. The previous explanation of the rise in the unsteady pressure near local sonic condition as a result of the *acoustic blockage* is essentially based on the mean flow inhibiting the propagation of the acoustic disturbances. In order to examine this physical phenomenon, we consider the case of a convergent-divergent nozzle with inlet disturbances propagating downstream and outlet disturbances propagating upstream. This simple model will isolate the basic effect of the *acoustic blockage* and will elucidate the essential features associates with the propagation of acoustic and other disturbances in unsteady transonic flows. The phenomenon of *acoustic blockage* by the mean flow can be readily understood by considering the expression of the intensity I of a plane acoustic wave propagating upstream of a flow with a velocity

U. In this simple case, $I = p'(c_0 - U)$, where p' is the acoustic pressure and c_0 is the speed of sound. If I is nearly constant and U increases while remaining subsonic, then p' would increase. Hence, when the mean flow Mach number is close to unity, upstream propagating acoustic disturbances are blocked and strongly amplified.

The computational model is based on PROUST, an unsteady Euler equations algorithm developed by Aubert (1993) and Ferrand and Aubert (1994). This code uses a MUSCL finite volume formulation over structured meshes. It is based on a Van Leer flux vector splitting with a hyberbolic tangent limiter to control spatial accuracy in the vicinity of discontinuities. The time discretization uses an explicit second-order Runge-Kutta scheme with five steps. Compatibility conditions are introduced at all boundaries to satisfy impermeability conditions at the solid boundaries and nonreflecting conditions at the inlet and oulet boundaries.

The geometry of the nozzle is two-dimensional and is identical to that used by Ott et al. (1993) in their experimental and computational investigation of the shock motion in a nozzle subject to downstream mechanical excitations. The nozzle has a 10% cross-section variation from inlet to throat. The computational domain is a rectangle representing one half of the nozzle, with dimensions of 2 in the streamwise direction and 0.4 in the cross-section direction. The nozzle occupies the central part of the computational domain and extends over a streamwise distance of 4/3. The grid lines in the streamwise direction follows an evolutionary law between the nozzle axis and its solid boundary. In the cross-sectional direction, the grid lines are vertical lines with concentration near the throat. The present computational results were validated by comparison with the data of Ott et al. (1993).

Two cases are investigated. One is subsonic with upstream Mach number $M_\infty = 0.64$. The Mach number in the throat cross-section varies from 0.90 along the axis to a maximum value $M_{max} = 0.97$ at the nozzle surface. The second case investigated is a transonic flow where $M_\infty = 0.66$, and the Mach number just upstream of the shock varies from 1.13 along the axis to a maximum value $M_{max} = 1.24$ at the nozzle surface. Figures 11 and 12 show the Mach contours for the subsonic and transonic cases, respectively. Sinusoidal disturbances are imposed at the inlet for the total pressure and at the outlet for the static pressure

$$p'^{(i)}_{t,s} = a_{t,s}\, sin\omega t \qquad (2)$$

where the supercript (i) denotes the initial imposed condition and the subscripts t and s denote total or static pressure, respectively. The reduced frequency is here defined as $k_1 = \omega d_i/2U_\infty$, where d_i is the nozzle diameter at the throat. For all calculations reported in this paper, k_1 was taken to be equal to 0.3. The amplitude of the oscillation $a_{t,s}$ is fixed at 0.2% of the mean pressure. In order to measure the rise of the unsteady pressure, the unsteady static pressure p'_s is normalized with respect to its inlet or outlet (a_s) magnitude. For an outlet imposed disturbance, Figure 13 shows the variation of $|p'_s|$ throughout the nozzle for three cross-section locations, one along the nozzle axis, the second along the streamwise grid line passing by the point 0.35 at the outlet, and the third along the nozzle surface. The corresponding M_{max} are 0.9, 0.95 and 0.97, respectively. We note the sharp rise in the unsteady pressure in the throat and particularly at the nozzle surface where its magnitude is about 14 times that of its value at the outlet. This sharp pressure rise is the result of the *acoustic blockage* of the upstream propagating acoustic waves by the near sonic mean flow.

When the disturbance is imposed at the inlet, the resulting unsteady pressure at the throat does not display such a significant pressure rise. Figure 14 shows a comparison between the unsteady normalized pressure magnitudes, $|p'_s|$, along the nozzle surface in response to inlet and outlet disturbances for the same subsonic flow. The unsteady pressure peak resulting from an outlet pressure disturbance is about 5 times that of the inlet disturbance. Figure 15 shows a similar comparison to that of Figure 14 except that the mean flow is now transonic with a shock downstream of the throat. In both cases, the shock motion has a small magnitude and only one grid point is affected. Improved accuracy can be obtained by a finer mesh structure near the shock. The pressure peaks for both disturbances occur at the foot of the shock rather than at the throat of the nozzle. For inlet disturbances, $|p'_s|$ is almost constant throughout the nozzle except at the shock location where it rises to about 3. For the outlet disturbance propagating upstream, $|p'_s|$ begins to rise downstream of the shock as in the subsonic case and then rises very sharply near the shock location. Upstream of the shock, $|p'_s|$ is practically nil since the disturbance cannot propagate through the supersonic region upstream of the shock and the motion of the shock is small. Thus, the nozzle model confirms the *acoustic blockage* model proposed for the cascade results.

4. Conclusions

An acoustic blockage model is proposed to explain the rise of the unsteady pressure magnitude along the surface of a cascade blade in transonic flow. The model is based on the concept that when the mean flow Mach number is close to unity, upstream propagating acoustic disturbances are blocked and strongly amplified. This concept has been successfully tested for a transonic convergent-divergent nozzle, a model problem, using nonlinear Euler calculations. For a cascade, the problem is certainly more complex because of the strong velocity gradient near the leading and trailing edges, and the fact that acoustic waves may or may *not* propagate upstream and/or downstream. However, the *acoustic blockage* appears to be the main cause of the unsteady pressure bulge near a shock or a high subsonic flow region.

The unsteady pressure bulge has a significant effect on the overall unsteady lift and moment. It also affects the flutter stability boundary and causes large local stresses which may result in high cycle fatigue failure. It is therefore advantageous to determine design conditions where this unsteady pressure bulge can be eliminated or reduced. Since it is caused by acoustic blockage, one might also consider active acoustic control as a means for eliminating this undesirable effect.

Acknowledgements

This work is supported by NASA Lewis Research Center under Grant NAG 732, monitored by Mr. Dennis Huff, and NATO Scientific Fellowship.

References

Atassi, H. M., 1994, "Unsteady Aerodynamics of Vortical Flows: Early and Recent Developments," *Aerodynamics and Aeroacoustics*," Editor K. Y. Fung, Chap. 4, pp. 119–169, World Scientific.

Atassi, H. M., Fang, J and Patrick, S., 1993, "Direct Calculation of Sound Radiated From Bodies in Nonuniform Flows," *Journal of Fluid Engineering*, Vol. 115, pp. 573–579

Aubert, S., 1993, "Etude de schemas a haute precision pour la simulation d'ecoulements transsoniques instationnaires ou visqueux. Application aux turbomachines," *Ph.D. Thesis*, Ecole Centrale de Lyon

David, S. S., and Malcolm, G. N., 1979, "Experiments in Unsteady Transonic Flow", AIAA Paper 79-769, *Proc. AIAA/ASME/ASCE/AHS 20th Structure, Structural Dynamics, and Material Conference*, ST. Louis, MO., pp. 192–208

David, S. S., and Malcolm, G. N., 1980, "Unsteady Aerodynamics of Conventional and Supercritical Airfoils", AIAA Paper 80-734, *Proc. AIAA/ASME/ASCE/AHS 21th Structure, Structural Dynamics, and Material Conference*, ST. Louis, MO., pp. 417–433

Fang, J. and Atassi, H. M., 1993a, "Numerical Solutions for Unsteady Subsonic Vortical Flows Around Loaded Cascades," *Journal of Turbomachinery*, Vol. 115, pp. 810–816

Fang, J. and Atassi, H. M., 1993b, "Compressible Flows with Vortical Disturbances Around a Cascade of Loaded Airfoils," *Unsteady Aerodynamics, Aeroacoustics, and Aeroelasticity of Turbomachines and Propellers*, Editor, H.M. Atassi, Springer–Verlag, pp. 149–176

Ferrand, P., 1986, "Etude theorique des ecoulements instationnaires en turbomachine axiale. Application au flottement de blocage,' *State Thesis*, Ecole Centrale de Lyon

Ferrand, P. and Aubert S., 1994, "A New Mixed Van Leer Flux Splitting for Transonic Viscous Flow", AIAA Paper 94-1876

Fransson, T. H. and Verdon, J. M., 1993, "Panel Discussion on Standard Configurations for Unsteady Flow Through Vibrating Axial–Flow Turbomachine–Cascades," *Unsteady Aerodynamics, Aeroacoustics, and Aeroelasticity of Turbomachines and Propellers*, Editor, H.M. Atassi, Springer–Verlag, pp. 859–889

Huff, D. L., Swafford, T. W. and Reddy, T. S. R., 1991, "Euler Flow Predictions for an Oscillating Cascade Using a High Resolution Wave-Split Scheme," ASME Paper GT-198

Ött, P., Bölcs, A. and Fransson, T. H., 1993, "Experimental and Numerical Study of the Time Dependent Pressure Response of a Shock Wave Oscillating in a Nozzle", ASME Paper 93-GT-139

Tijdeman, H., 1977, "Transonic Flow Past Oscillating Airfoils", *NLR TR 77090 U*, NLR, Amesterdam, the Netherlands

Tijdeman, H. and Seebass, R., 1980, "Investigations of the Transonic Flow Around Oscillating Airfoils", *Ann. Rev. Fluid Mech.* 12, pp. 181–222

Verdon, J. M., Huff, D. L. and Ayer, T. C., 1993, Personal Communication

Verdon, J. M. and Hall, K. C., 1990, "Development of a Linearized Unsteady Aerodynamic Analysis for Cascade Gust Response Predictions", NASA Contractor Rep. 4308

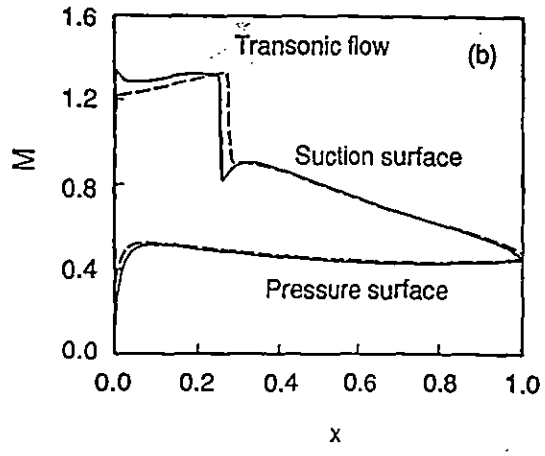

Figure 1: Blade Surface Mach Number Distribution for the Tenth Standard Configuration cascade in transonic flow. M_∞=0.8, $\Omega_{-\infty} = 58°$

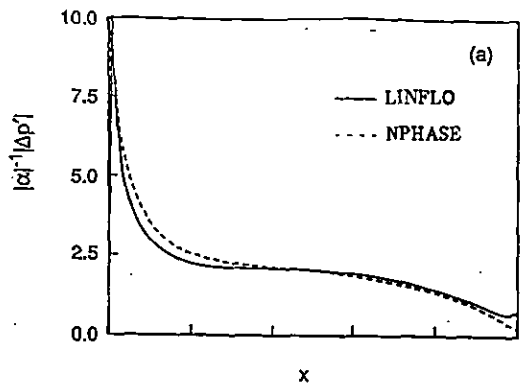

Figure 2: Magnitude of the first harmonic unsteady pressure difference distribution for the Tenth Standard Configuration cascade undergoing an in-phase torsional oscillation of amplitude α=2° at $k_1 = 0.5$ about midchord. $M_\infty = 0.7$, $\Omega_{-\infty} = 55°$.

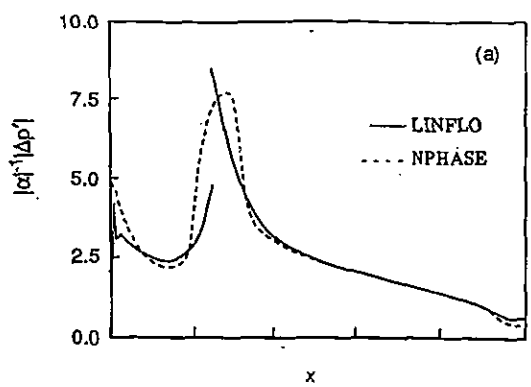

Figure 3: Magnitude of the first harmonic unsteady pressure distribution for the Tenth Standard Configuration cascade undergoing an in-phase torsional oscillation of amplitude α=2° at $k_1 = 0.5$ about midchord, $M_\infty = 0.8$, $\Omega_{-\infty} = 58°$

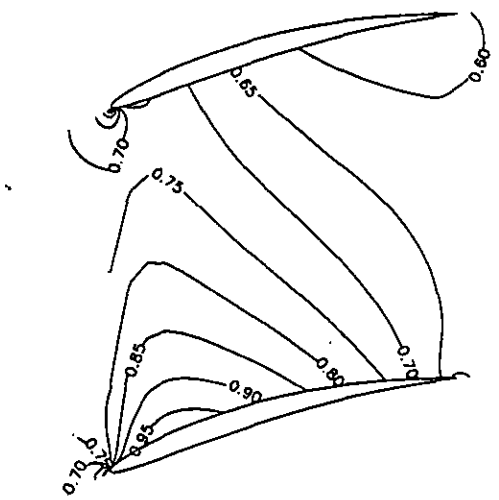

Figure 4: Cascade geometry and the Mean flow Mach number contours for case 1

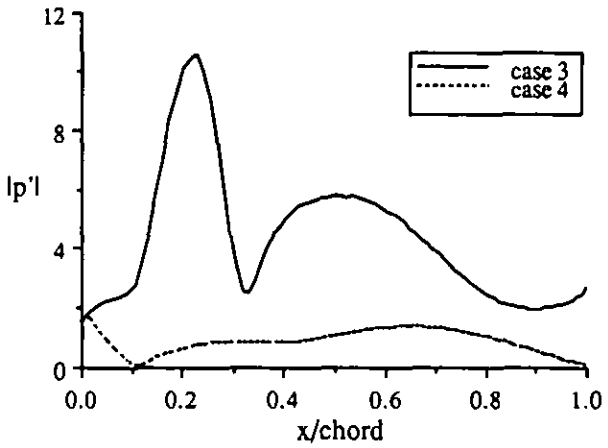

Figure 7: Magnitude of the unsteady pressure distribution along the suction surface of the blade for cases 3 and 4 at $k_1 = 4.35$

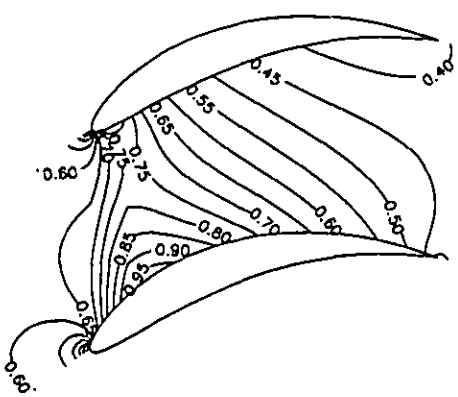

Figure 5: Cascade geometry and the Mean flow Mach number contours for case 3

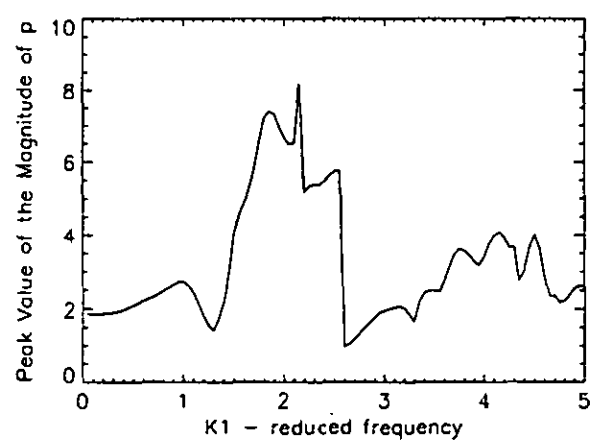

Figure 8: Peak of the magnitude of the unsteady pressure vs. k_1 for case 1 in the region where M_{max} occurs

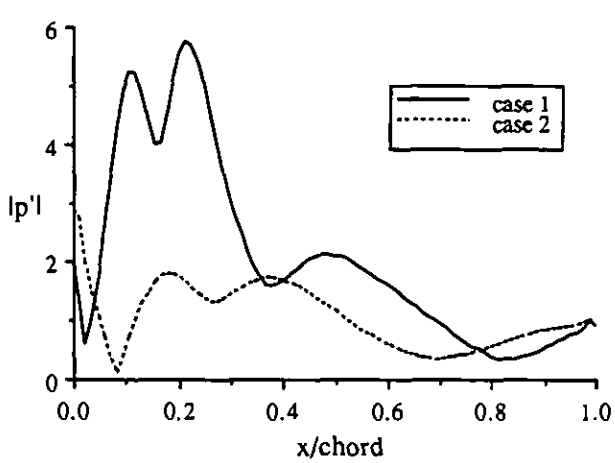

Figure 6: Magnitude of the unsteady pressure distribution along the suction surface of the blade for cases 1 and 2 at $k_1 = 2.5$

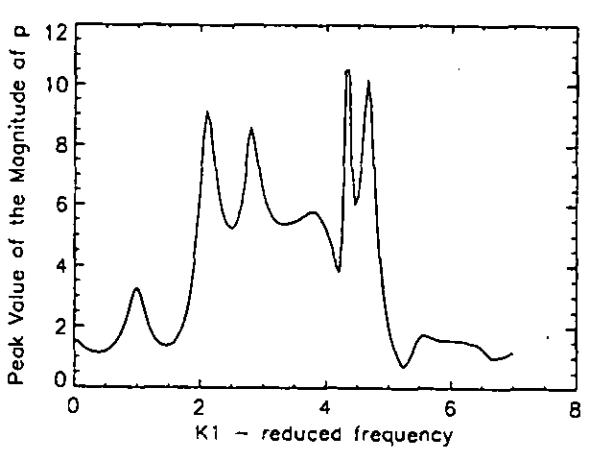

Figure 9: Peak of the magnitude of the unsteady pressure vs. k_1 for case 3 in the region where M_{max} occurs

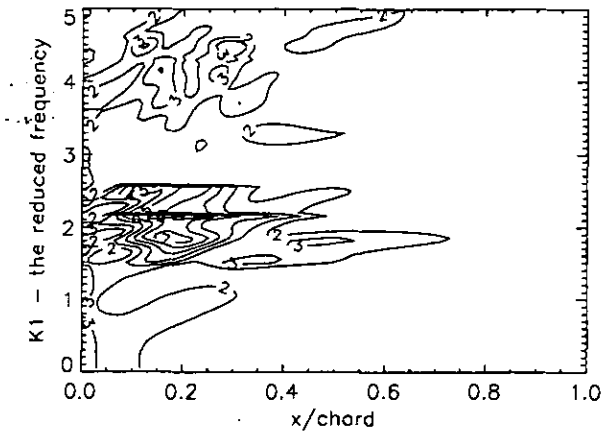

Figure 10: Contours of the magnitude of the unsteady pressure along the blade suction surface vs. k_1 for case 1

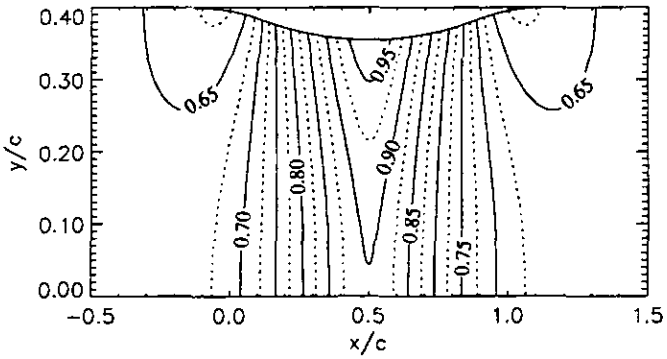

Figure 11: Nozzle geometry and the mean flow Mach number contours for the subsonic case

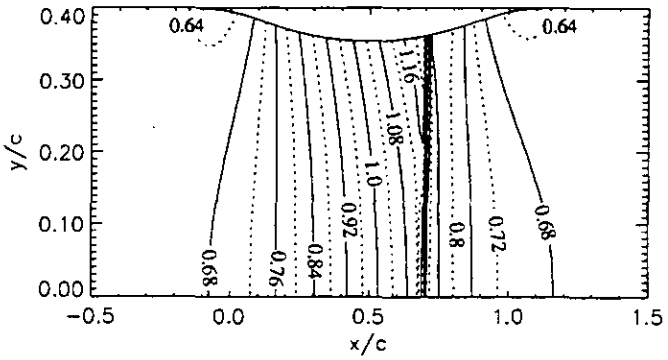

Figure 12: Nozzle geometry and the mean flow Mach number contours for the transonic case

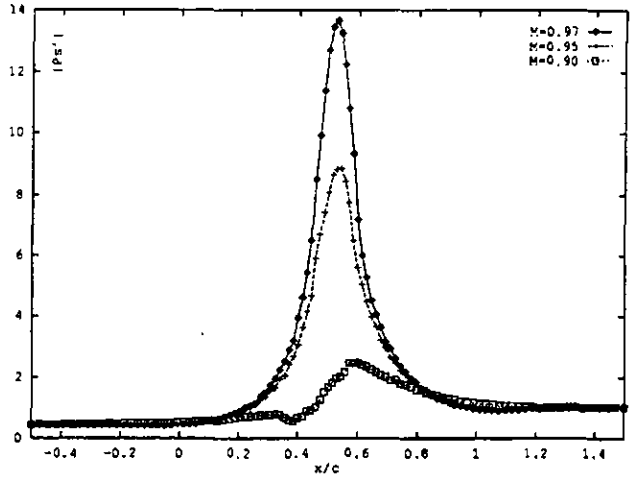

Figure 13: Magnitude of the unsteady pressure distribution for three cross-section locations for the subsonic nozzle case at $k_1 = 0.3$

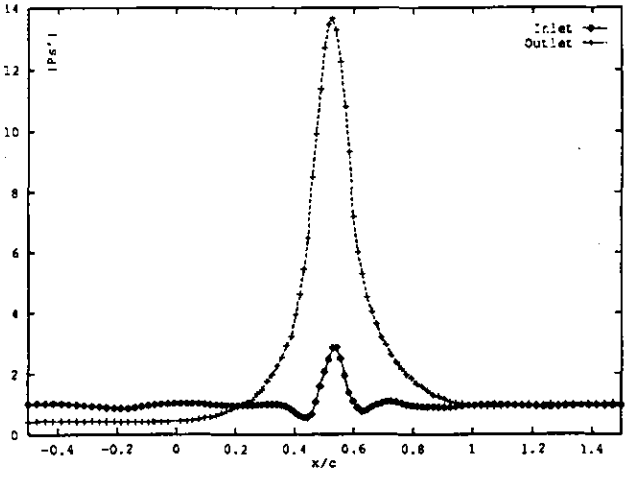

Figure 14: Magnitude of the unsteady pressure distribution along the nozzle surface for inlet and outlet disturbances for the subsonic nozzle case at $k_1 = 0.3$

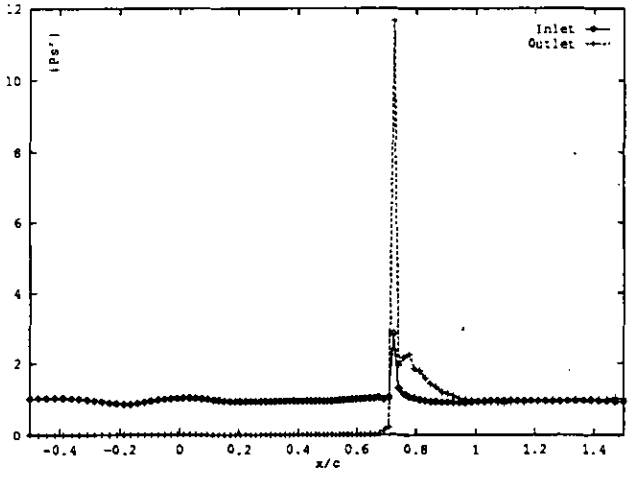

Figure 15: Magnitude of the unsteady pressure distribution along the nozzle surface for inlet and outlet disturbances for the transonic nozzle case at $k_1 = 0.3$